Natural Hazards and Earth System Sciences (2003) 3: 321–332

Natural Hazards and Earth System Sciences

Simulation of the trans-oceanic tsunami propagation due to the 1883 Krakatau volcanic eruption

B. H. Choi[1], E. Pelinovsky[2], K. O. Kim[3], and J. S. Lee[1]

[1]Department of Civil and Environmental Engineering, Sungkyunkwan University, Suwon, 440-746, Korea
[2]Laboratory of Hydrophysics and Nonlinear Acoustics, Institute of Applied Physics, 46 Uljanov Street, 603950, Nizhny Novgorod, Russia
[3]Research Center for Disaster Environment, DPRI, Kyoto University, Gokasho, Uji, Kyoto, 611-0011, Japan

Received: 13 June 2002 – Revised: 16 September 2002 – Accepted: 8 October 2002

Abstract. The 1883 Krakatau volcanic eruption has generated a destructive tsunami higher than 40 m on the Indonesian coast where more than 36 000 lives were lost. Sea level oscillations related with this event have been reported on significant distances from the source in the Indian, Atlantic and Pacific Oceans. Evidence of many manifestations of the Krakatau tsunami was a subject of the intense discussion, and it was suggested that some of them are not related with the direct propagation of the tsunami waves from the Krakatau volcanic eruption. Present paper analyzes the hydrodynamic part of the Krakatau event in details. The worldwide propagation of the tsunami waves generated by the Krakatau volcanic eruption is studied numerically using two conventional models: ray tracing method and two-dimensional linear shallow-water model. The results of the numerical simulations are compared with available data of the tsunami registration.

1 Introduction

A most devastating tsunami occurred when the volcano on the Krakatau Island, situated in the Sunda Strait between Java and Sumatra (Fig. 1) erupted in August 1883 (Simskin and Fiske, 1983; Bryant, 2001). Four largest explosions of this volcano in 26–27 August produced tsunami waves recorded on the coasts of the Sunda Strait. These waves are generally attributed to submarine explosion, caldera's collapse and pyrolastic flow entering the sea (Francis, 1985). On 26 August about 17:00 LT, loud explosions recurred at intervals of 10 min, and a dense tephra cloud rose 25 km above the island. Small tsunami waves 1–2 m in height swept the Sunda Strait. On the morning of 27 August, three horrific explosions occurred. The first explosion at 05:28 LT destroyed the 130 m peak of Perboewatan on the Krakatau Island (now it does not exist), forming a caldera that immediately infilled with seawater and generated a tsunami. At 06:36 LT, the 500 m-high peak of Danan (also does not exist) exploded and collapsed, sending more seawater into the molten magma chamber of the eruption and producing another tsunami up to 10 m. The third blast, at 09:58 LT, tore the remaining part of the Krakatau Island (Rakata Island) apart. Including ejecta, 9–10 km^3 of solid rock was blown out of the volcano. About 18–21 km^3 of pyrolastic deposits spread out over 300 km^2 to an average depth of 40 m. Fine ash spread over an area of 2.8×10^6 km^2, and thick pumice rafts impeded navigation in the region up to five months afterwards. A caldera with 6 km in diameter and 270 m deep formed where the central island had once stood. The third blast was the largest sound ever heard by humanity and was recorded 4800 km away. The atmospheric shock wave traveled around the world seven times. Barometers in Europe and the United States measured significant oscillations in pressure over nine days following the blast. The total energy released by the third eruption was equivalent to 200 megatons atomic bomb (8.4×10^{17} joules).

The two predawn blasts each generated tsunami that drowned thousands in the Sunda Strait. The third blast-induced wave was cataclysmic and devastated the adjacent coastline of Java and Sumatra. The northern coastline of the eruption was struck by waves with a maximum runup height of 42 m (town of Merak, see Fig. 1), and tsunami penetrated 5 km inland over low-lying areas. Great amplification of the tsunami waves in Merak (from 15 m to 42 m) is related due to the tunnel-shaped bay. At least 36 000 people were killed, most by the sea waves, and 300 villages were destroyed. Sea surface oscillations have been recorded worldwide: the Indian Ocean (Indonesia, India, Sri Lanka, Yemen, Mauritius, South Africa, Australia), the Pacific (USA, New Zealand, Japan and Chile), the Atlantic (France, Antilles, Panama and South Georgia Islands), see Fig. 2. Various descriptions of tsunami wave manifestation (both, eyewitness and tide-gauge records) and corresponding scientific accounts are collected by Simskin and Fiske (1983).

Numerical simulation of the tsunami propagation in the Sunda Strait around the Krakatau Island using the ray method

Correspondence to: E. Pelinovsky
(enpeli@hydro.appl.sci-nnov.ru)

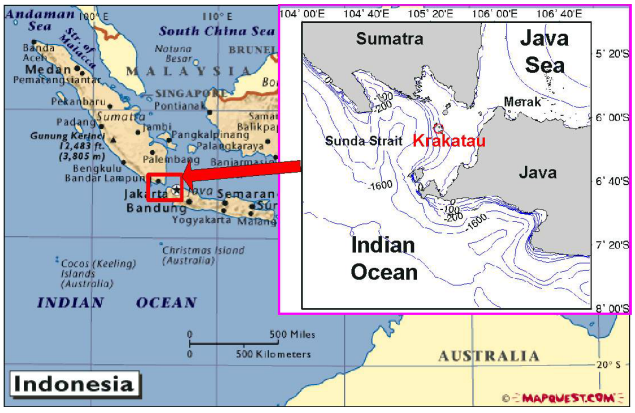

Fig. 1. Location of the Krakatau Island.

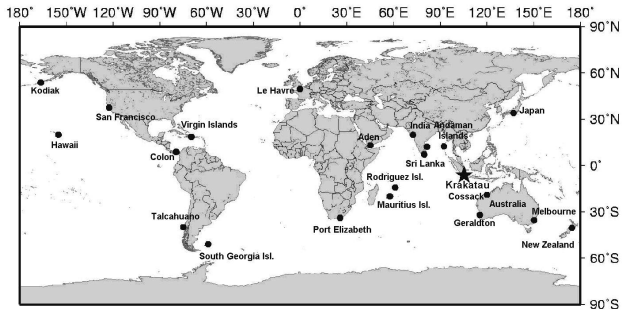

Fig. 2. The locations of the 1883 Krakatau tsunami recording.

has been performed by Yokoyama (1981). The wave heights were calculated using the Green's law based on the energy flux conservation. Then Nakamura (1984) repeat these calculations using the finite-difference scheme. He simulated also the tsunami wave propagation in the adjacent part of the Indian Ocean and the comparison with the observed data leads to the estimated depth in the equivalent tsunami source in 700 m. The Krakatau tsunami was also numerically simulated by Kawamata et al. (1992) for the region of outside the Sunda Strait by assuming the caldera formation, which makes the surrounding water rush into the cavity. Nomanbhoy and Satake (1995) investigated the mechanism of the tsunami generation at the Krakatau volcanic eruption. Based on the numerical simulation of the near field (Java and Sumatra) they concluded that the submarine explosion model as the source of the largest tsunami is favored.

The arrival time of the tsunami in the numerous ports of World Ocean has been estimated in several years after the Krakatau event based on the existing tide-gauge records (35) and eyewitness accounts, and, very roughly, on the long wave theory for the wave speed (cited on Simskin and Fiske, 1983). In many places the sea level disturbance were weak, "no precise or close comparison between various tidal diagrams can be made, and this doubt of the identification of any particular wave at different places, causes much uncertainty in the result, as far as it relates to the speed of waves". This concerns mainly Pacific and Atlantic data, which probably had no connection with the Krakatau event.

Ewing and Press (1995) analyzing historic data have noticed, "tide-gauge disturbances at distant stations correlate in time with the first aerial wave arriving at the station" and suggested new hypothesis of the origin of the sea level disturbances at distant stations based on coupling between the barometric disturbance and the ocean surface wave. Then Press and Harkrider (1966) and Garret (1976) developed this mechanism and obtained the satisfactory agreement for wave amplitudes in the USA coastal stations. Probably, the sea level disturbances in New Zealand (in particular, in Lake Taupo not connected to the ocean) were also related with the atmospheric pressure waves (Bryant, 2001).

The present paper considers the direct tsunami wave propagation from the Krakatau volcanic eruption in the framework of the shallow water theory to analyze the contribution of this mechanism for an explanation of the observed sea level disturbances. Main goal of this study is to perform the numerical simulation of the tsunami waves on globe using the detailed bathymetry of the World Ocean. It can obtain more rigorous estimates of the tsunami travel time, clarify the role of the tsunami pathways through the Antarctic basin, and compare the wave characteristics in different areas. The material is organized as follows. The available data of the tsunami waves from the Krakatau events is briefly summarized in Sect. 2. The ray tracing method allowed to calculate the pathways on the globe is described in Sect. 3 and it is applied to determine the travel time of the leading wave. The direct numerical simulation of the tsunami wave propagation is performed in the framework of two-dimensional linear shallow-water theory; see Sect. 4. The hydrodynamic model is applied to describe characteristics of the tide-gauge records, and to improve computed values for tsunami travel time. The applicability of hydrodynamic model to describe the observed sealevel disturbances related with tsunami waves generated at the Krakatau volcanic eruption is discussed in conclusion.

2 Tsunami wave descriptions

Various data of the 1883 tsunami manifestation are collected in the books by Simskin and Fiske (1983), Murty (1977), Bryant (2001). Also some data are presented in Russian Navy Atlas (USSR Navy, 1974) and in unpublished manuscript by Soloviev and Go (1974). The locations of places where tsunami waves were observed are presented in Fig. 2. On the coasts of the Sunda Strait the wave height reached 15 m in average with maximum up to 42 m. Our focus is to study the far-field tsunami propagation from the Krakatau volcanic eruption only. Data of the tsunami observations on long distances from the Krakatau is briefly reproduced, revised and discussed, as follows:

On Andaman Islands, India (Port Blair, 2440 km from the Krakatau, Fig. 3), the weak tsunami was recorded on the tide-gauge station and no data of tsunami manifestation on

Fig. 3. The locations of tsunami observations in India and Sri Lanka.

the coast. The quality of the tide-gauge record is not very high to determinate the wave characteristics. According to received opinion, the wave height is reached 0.2 m. The first wave arrived at 14:00 LT (15:30 of the Krakatau time), and the characteristic wave period is about 1 h. The travel time can be estimated as 4 h. We will show this tide-gauge record in Sect. 4 comparing with computing data.

On Sri Lanka (3113 km from the Krakatau) two descriptions of tsunami on 27 August are available. In Galle (southwestern coast, see Fig. 3), "an extraordinary occurrence was witnessed at the wharf at about 01:30 LT (15:00–15:30 of the Krakatau time). The sea receded at far as the landing stage on the jetty. The boats and canoes moored along the shore were left high and dry for about three minutes. A great number of prawns and fishes were taken up by the coolies and stragglers about the place before the water returned. Since the above was written, the sea has receded twice throughout the harbour". At Negombo (north from Colombo, Fig. 3), at 03:00 LT (16:30–17:00 of the Krakatau time). "The rise of the tide was so much above the usual water-mark that many of the low morasses lying in close proximity to the seaside were replete with water that flowed into them. However, the water thus accumulated did not remain long, but, forming into a stream, wended its course in a southerly direction, through low lands, to a distance of nearly a quarter of a mile, and found a passage back to the sea; thus the water that had so abruptly covered up such an extent of land did not take many days in draining off." "The receding waters were not slow behind in their action, for they washed away a belt of land about 132-198 feet (40.23–60.35 m) in extent, including the burial ground situated on the coast to the south-west of the bay compelling the inhabitants to seek shelter in a neighboring cocoa-nut garden". Sixteen recessions were counted between noon and 03:00 LT on 27 and the rushing water produced what was described as a hissing sound. At Arugam Bay (southeastern coast, Fig. 3), "Three moorwomen, three children, and a man were crossing the bar about 03:00 LT. A big wave came up from the sea over the bar and washed them inland. Soon after the water returned to the sea. The man said that the water came up to his chest: he is a tall man. These people were tumbling about in the water, but were rescued by people in boats who were fishing in the Kalapuwa (inland estuary). The lost the paddy they were carrying, and one of the women died two days after of her injuries".

From these descriptions we can conclude that tsunami on Sri Lanka presents the group from 16 waves with average period of 11 min, and its crest height is more than 1 m. The reported first wave is positive or negative depending from the location. The wave has approached to the coast 5–7 h after origin.

Tide-gauges records at many ports in India show the sea level disturbances. In particular, tide-guages records at Madras and Negapatam (see, Fig. 3) have a period of about 1.0 to 1.5 h. The wave amplitude at Negapatam station was 0.56 m. An extraordinary phenomenon of tides was witnessed at Bandora near Bombay (4500 km and 11 h from the Krakatau), on the morning of 28 August (there is probably the mistake on p. 147 of the book by Simskin and Fiske (1983), because the Krakatau time of this event is 21:00 LT on 27 August as cited in the same book on p. 43. The local time should be 19:00 LT on 27 August) by those who were at the time on the seashore. "The tide came in, at its usual time and in a proper way. After some time, the reflux of the tide went to the sea in an abrupt manner and with great impetus, and the fish, not having sufficient time to retire with the waves, remained scattered on the seashore and dry places, and the fishermen, young and old, had a good and very easy task to perform in capturing good-sized and palatable fish, without the least trouble or difficulty, to their hearths' content, being an extraordinary event never seen or heard of before by the old men; but suddenly the flux came with a great current of water, more swift than horse's running. The tide was full as before, and this flux and reflux continued two or three times, and at least returned by degrees as usual". So, tsunami in India began from the fast ebb, and two-three waves with steeper slopes were reported; the period of such waves should be 10 min or more, looking on description of the people behavior.

"The great tidal disturbance" at Aden occurred 12 h after the Krakatau volcanic eruption, on distance of 3800 nautical miles (7038 km). The observed wave amplitude on tide-gauge record is 0.24 m.

On Rodriguez Island in the Indian Ocean (4653 km from the Krakatau and 1600 km east of Madagascar) the tsunami effects were observed starting from 27 August 13:30 LT

(16:30 of the Krakatau time). "It was ebb tide, and most of the boats were aground. The sea looked like water boiling heavily in a pot, and the boats, which were afloat, were swinging in all directions. The disturbance appeared quite suddenly, lasted about half an hour, and ceased as suddenly as it had commenced. At 14:20 LT a similar disturbance began; the tide all of a sudden rose 5 feet 11 inches (1.8 m), with a current of about 10 knots an hour (1.85 km/h) to the westward, floating all boats, which had been aground, and tearing them from their moorings. All this happened in a few minutes. The tide then turned with equal force to the eastward, leaving the boats which were close in-shore dry on the beach, and dragging the Government boat (a large decked pinnace) from heavy moorings, and leaving it dry on the reefs. The inner harbour was almost dry. The water in the channel was several feets below the line of reefs; and, owing to the sudden disappearance of the water, the reefs looked like islands rising out of the sea. The tides continued to rise and fall about every half hour, but not so high, or with the same force, as the first tide. By noon on the 29 August, the tide was about its usual height".

So, tsunami presents the wave group with the period of 30 min and the total duration about two days. Several waves have the same amplitudes and at least the first waves have steep fronts (duration of a few minutes) like shock waves. The crest height is 1.8 m and the through amplitude is approximately the same, therefore, the wave height is 3.6 m. Wave velocities were about 5 m/s and this corresponds to the relation from linear theory for the depth about 2 m. The tsunami waves have approached 6–7 h after origin.

On Mauritius Island in the Indian Ocean (5445 km from the Krakatau) tsunami was observed at the same time. "At about 13:30 LT the water came with a swirl round the point of the sea wall and in about a couple of minutes returned with the same speed. This took place several times, the water on one occasion rising 2.5 feet (0.76 m)". In another place (funnel-shaped harbor) "the water, which was then unusually low, suddenly rushed in with great violence, rising fully 3 feet (0.91 m) above the former level. An alternate ebb and flow then continued till nearly 19 h, and the interval between high and low water were about 15 min. There was no high wave or billow, but strong currents, the estimated velocity of which was about 18 knots an hour. Vessels moored near the Dry Docks swayed much and at about 18:30 LT one of the hawsers of the Touared, 10 inches in circumference, parted. Buoys in the neighborhood were at times seen spinning round like tops. Disturbances were observed on 28 August also, and there unusual currents even on the 29 August".

So, characteristics of tsunami waves on the Mauritius and Rodriguez Islands (arriving time, the wave period, wave amplitudes) are almost the same.

On South Africa, Port Elizabeth (7546 km from the Krakatau), the first tsunami wave has approached approximately at 16:00 LT (23:30 of the Krakatau time) on 28 August and the maximal wave 4 h later with height about of 1.4 m. The sea level oscillations with visible period of 1 h continued during next day. This tide-gauge record will be shown in Sect. 4. The travel time of the first wave is estimated as 13.5 h.

In Australia, within four hours of the final eruption, a tsunami arrived at North-West Cape, 2100 km away (Bryant, 2001). The wave swept through gaps in the Ningaloo Reef and penetrated 1 km inland over sand dunes. Nakamura (1984) pointed out, the sudden sea waves with maximum disturbance of 1.5 m came to Cossack (northwestern part) on 27 August at 16:00 LT (15:15 of the Krakatau time). At Geraldton (southwestern part), the sea level drew down to 1.8 m suddenly at 20:00 LT (19:00 of the Krakatau time) on the same day. In Williamstown (near Melbourne) the wave approached at 04:40 LT on 28 August (01:40 of the Krakatau time). In Tasmania, the fast arriving of the tidal wave in the Huon River (south of Hobart) arrived with large speed and force on August 28 and 29; this flow lifted the rubbish on the height 1 m (Soloviev and Go, 1974). The wave approached to the northwestern shelf of Australia for 5 h and then propagated along the Australian coast for 10 h.

On New Zealand (7767 km from the Krakatau), in Auckland Harbor at 04:00 LT on 29 August (23:00 on 28 August of the Krakatau time), "in a few minutes the tide rose fully 1.8 m and as suddenly receded again, leaving the vessels in port high and dry. Throughout the day the way was felt several times with equal strength". Additional information is in the unpublished manuscript by Soloviev and Go (1974). In Timaru (eastern coast of the South Island), several waves were pointed in the morning of 29 August. Also the water rose and fell twice for 40 min in the Lake Taupo (center of the North Island) with amplitude 0.5 m. If the date, August 29 is correct, the travel time is about of 37 h.

The tide-gauge record at Le Havre, France (17960 km from the Krakatau) shows the sea level disturbances at 21:35 on 28 August (the Krakatau time), 32.5 h after the Krakatau volcanic eruption. The wave height is week, about 12 mm.

In USA the sea level disturbances can be detected on the tide-gauges at San Francisco, Kodiak and Honolulu, which will be given in Sect. 4. At Sacramento (San Francisco), the first oscillations appeared at 11:00 LT on 27 August (02:00 on 28 August of the Krakatau time), and the maximal wave up to 0.1 m – 2 h later, at 13:00 LT (04:00 on 28 August of the Krakatau time), and the travel time of the first wave can be estimated as 16 h. At St. Paul's (Kodiak), small waves (0.1 m) were recorded between 17:00 LT and 23:00 LT on 27 August (09:00–15:00 on 28 August of the Krakatau time). The travel time of the first wave is estimated as 23 h. At Honolulu, sea level disturbances began at 03:00 LT on 27 August (20:00 on the same day of the Krakatau time) and continued two days. Maximal wave approached 2 h later and had a height of 0.25 m. The travel time of the first wave can be estimated as 10 h. On the Caribbean Sea, Virgin Islands, at St. Thomas, "A tidal wave occurred on 27 August, the water receded from the shore three times" (Lander et al, 2002). At Colon (Panama Canal), the tide-gauge record shows wave disturbances with the height up to 0.4 m. The first negative wave approached at 15:00 LT on 27 August (03:30 on 28 Au-

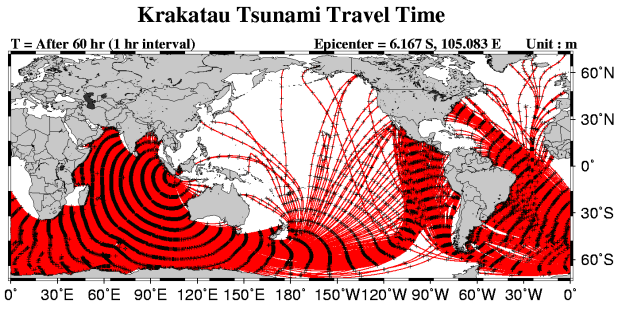

Fig. 4. Krakatau tsunami travel time chart computed from ray-tracing tsunami model.

gust of the Krakatau time), and the maximal wave – 1.5 h later. The travel time of the first wave is 17.5 h.

On South Georgia Islands (Moltke Harbour), tsunami began at 14:00 LT on 27 August (23:00–24:00 on the same day of the Krakatau time), and the maximal wave arrived 12 h later, its height is about 0.3 m (tide-gauge record will be given later). The travel time of the first wave is estimated as 13–14 h.

The additional information of tsunami manifestation in the Pacific is presented on the map from the Russian Navy Atlas (USSR Navy, 1974) prepared by Sergey Soloviev, these locations shown in Fig. 2). First of all, the observations of tsunami with the height of 1 m on the coast of Japan should be pointed (Bryant, 2001 mentions that tide-gauges in Japan measured changes of 0.1 m). In Chile, Talcahuano, the difference between the maximal and minimal water level during 1 h reached 0.7 m at 08:00 LT, 28 August (20:00 of the Krakatau time, or 34 h after the volcanic eruption). Time is indicated in the unpublished manuscript by Soloviev and Go (1974); in their catalogue there is only general information that tsunami affected also to the sea level on the South American coast, and the sea level disturbances were 0.5 to 1 m (Soloviev and Go, 1974; Nakamura, 1984). On the Cape Horn (southern cape of America), the wave amplitude on the tide-gauge is 0.25 m. Ewing and Press (1995) gives arriving time for the first wave, 14:20 LT on 27 August (16.5 h after the volcanic eruption), and for the first great wave, 7.5 h later. Weak tidal phenomenon was pointed in 1883 on the Islas Tres Marias, Mexico, and Soloviev and Go (1974) consider this as tsunami from the Krakatau.

Russian Navy Atlas (USSR Navy, 1974) summarizes also data of tsunami observations in Java Sea (up to 3 m, near the Sulawesi Island, 0.5 m) and Cocos Islands, 1.5 m, but we were not able to find descriptions of these observations in the literature.

In the next sections numerical models will be used for explanation of the observed data (travel time, height) of the tsunami origin at the Krakatau volcanic eruption.

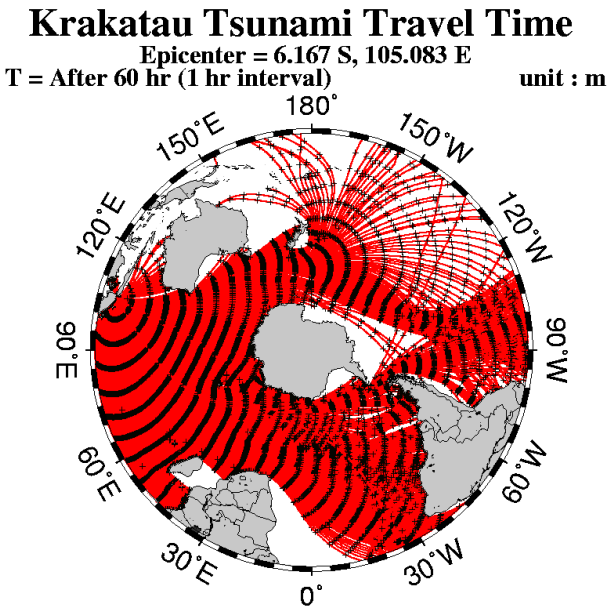

Fig. 5. Tsunami pathways through the circumpolar sea.

3 Ray tracing model

The ray tracing method is usually used as a short wavelength approximation in the theory of the long wave propagation in the smooth inhomogeneous media. Ray method leads to calculate directly the travel time and the wave amplitude using the Green's law based on the energy flux conservation. For tsunami waves this method is actively applied, including the 1883 Krakatau event (see, for instance, Simskin and Fiske, 1983). Below the formulating of the ray method for the spherical earth developed by Satake (1988) will be used. Ray tracing equations are:

$$\frac{d\theta}{dt} = \frac{\cos\zeta}{nR}, \tag{1}$$

$$\frac{d\phi}{dt} = \frac{\sin\zeta}{R\sin\theta}, \tag{2}$$

$$\frac{d\zeta}{dt} = \frac{\sin\zeta}{n^2R}\frac{\partial n}{\partial\theta} + \frac{\cos\zeta}{n^2R\sin\theta}\frac{\partial n}{\partial\varphi} - \frac{\sin\zeta\cot\theta}{nR}, \tag{3}$$

where θ and φ are latitude and longitude of the ray, $n = (gh)^{-1/2}$ is the slowness, g is the gravity acceleration, $h(\theta, \varphi)$ is the water depth, R is the radius of the Earth, and ζ is the ray direction measured counter-clockwise from the south. The above equations are solved by the Runge-Kutta-Gill method. Integration is performed by the midpoint method, using interpolated velocities; the detail of the method parallels that of Sobel and von Seggern (1978). Visualization of numerical results is discussed by Choi et al. (1997).

The location of the source in the numerical simulations almost coincides with the location of the Krakatau volcano, its coordinates are 6°10′ S, 105°10′ E, and depth in the source is 400 m. The number of rays is 3600 and they are initially distributed uniformly. For correct calculation of the travel

Table 1. Travel time of the first tsunami wave

Point	Observed time, h	Calculated time, h
Port Blair, Andaman Islands	4	4.5
Galle, Sri Lanka	5	4.5
Negombo, Sri Lanka	7	5
Bombay, India	11	8.6
Aden	12	10.17
Rodriguez Islands	6.5	6.67
Mauritius Islands	6.5	7.3
Port Elisabeth, South Africa	13.5	12
Cossack, Australia	5.25	3
Geraldton, Australia	9.25	4
Williamstown, Australia	15.6	8.5
Auckland, New Zealand	37	12.7
Havre, France	31.5	31.7
San Francisco, USA	16	26
Kodiak, Alaska, USA	23	27.7
Honolulu, Hawaii, USA	10	23
Colon, Panama	17.5	17
Port Mollke, South Georgia Is.	13.5	17
Talcahuano, Chile	34	21.5

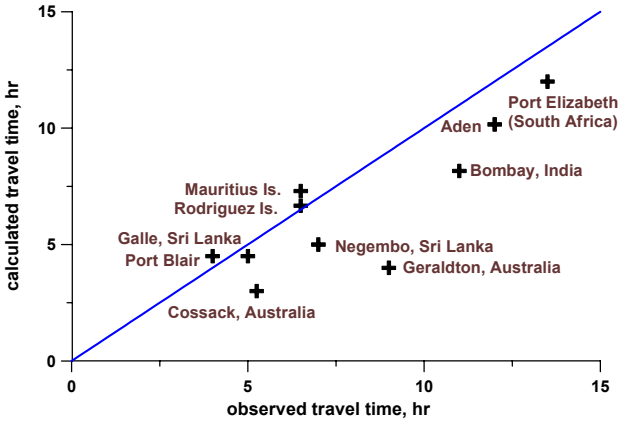

Fig. 6. Comparison of the observed and calculated travel times of the first wave in the basin of the Indian Ocean.

time some additional rays were used. The bathymetry is taken from the 2-min ETOPO2 dataset (Smith and Sandwell, 1997).

Results of computing of the tsunami pathways are shown in Fig. 4. Tsunami waves affect a whole basin of the Indian Ocean, and also they pass into the Pacific and Atlantic Oceans. These two pathways are well shown in Fig. 5; one way is the propagation to the Atlantic Ocean between Antarctic and South Africa, and another one is the propagation to the Pacific between Antarctic and Australia and also between Antarctica and Southern America. Most of energy passed to the Atlantic Ocean to compare with the Pacific Ocean. Early such pathways were not calculated because Antarctic waters were unsurveyed. Also the transmission of the tsunami energy over these paths is doubtful (Ewing and Press, 1995; Simskin and Fiske, 1983). Using numerical modeling with good sea-floor topography the tsunami pathways can be calculated with high accuracy. The results of the performed calculations show that the tsunami waves affect the coasts of the Indian Ocean, and the waves approach to the South America, both, Atlantic and Pacific coasts. The North America is more protected from the Krakatau tsunami, and the ray density determined the wave amplitude is relatively small. Other areas in the Pacific (western coast) and Atlantic (European coast) are almost not affected by tsunami. Also, it can be noted that waves do not pass significantly through the Indonesian archipelago into the Pacific, and this is a natural barrier for tsunami.

The ray tracing method allows calculating the tsunami travel time; these isochrones with 1 h interval are shown in Fig. 4. The calculated travel times can be compared with observed values for the first (leading) wave, given in Sect. 2. Calculated and observed travel times are summarized in Table 1. First of all the comparison can be done for the coast of the Indian Ocean (Fig. 6). The agreement is quite well, mainly for points, where the tsunami waves approach on the frontal direction (southern coast of Sri Lanka, Mauritius and Rodriguez Islands, Aden, Port Elizabeth). The western coast of Sri Lanka and India is in the "dark" zone of the ray pattern. Here another scenario of the tsunami waves propagation in the form of the edge waves should be realized, and the actual arriving time should be increased, as it is observed for Negombo and Bombay. The same effect have to be important for the Australian points where the observed travel time is also large to compare with ray predictions. For instance, this difference reaches 7 h for the tsunami waves at Williamstown (near Melbourne), see, Table 1. Our calculations in the framework of the ray tracing method do not take into account the wave propagation in the form of the edge waves leading to increase the tsunami travel time. Formally, the large travel time to compare with prediction of the ray theory is no contradiction because sometimes the first waves are not visible.

For transoceanic tsunami propagation the comparison of observed and calculated travel times is presented in Fig. 7. Surprisingly, the calculated arrived time for Le Havre, France is the same as the observed one, meanwhile the wave passed almost 18 000 km. Relative small disagreement is for Port Molke, South Georgia Islands and for St. Paul's, Kodiak, approximately 3–4 h. Maximal disagreement is for the New Zealand data where observed time is too large to compare with calculated one. Also the tsunami waves should arrive in Talcahuano (Chile) 12 h early that it is observed. In Honolulu, San Francisco and Panama the tsunami waves came significantly early that it is expected according to the ray theory. It means that such "early" disturbances cannot be connected with the direct sea wave propagation from the Krakatau Island. This was concluded early using the rough estimation of the tsunami travel time (Simskin and Fiske,

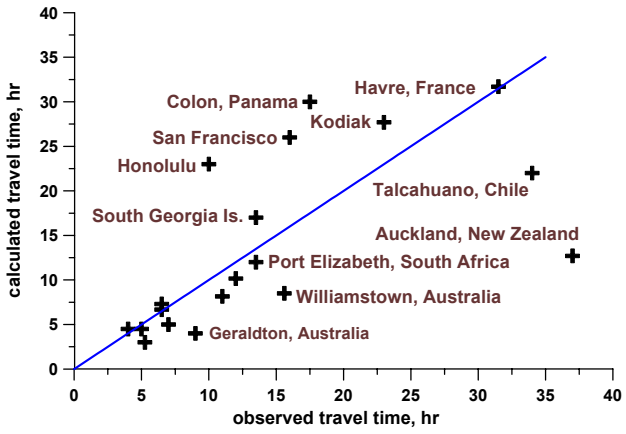

Fig. 7. Comparison of the observed and calculated travel times of the first wave in globe.

1983) and here confirmed using detailed numerical simulations on the 2 min bathymetry. The existing of such disturbances is assumed with the impact of the significant acoustic-gravity waves in the atmosphere generated at the volcano explosion on the sea surface and possible coupling between two wave systems (Ewing and Press, 1995; Press and Harkrider, 1966; Garret, 1976; Lander and Lockridge, 1989).

4 Hydrodynamic long wave modeling

As it is known the ray tracing method is effective only to calculate the travel time, but not the wave amplitude. For evaluation of the tsunami parameters, its transoceanic propagation from the Krakatau volcanic eruption is studied in the framework of the linear shallow water theory on the spherical earth,

$$\frac{\partial \eta}{\partial t} + \frac{1}{R\cos\theta}\left\{\frac{\partial M}{\partial \varphi} + \frac{\partial}{\partial \theta}(N\cos\theta)\right\} = 0, \quad (4)$$

$$\frac{\partial M}{\partial t} + \frac{gh}{R\cos\theta}\frac{\partial \eta}{\partial \varphi} = fN, \quad (5)$$

$$\frac{\partial N}{\partial t} + \frac{gh}{R\cos\theta}\frac{\partial \eta}{\partial \theta} = -fM. \quad (6)$$

where $M(\theta, \varphi, t)$ and $N(\theta, \varphi, t)$ are the flow discharges in meridional and zonal directions, $\eta(\theta, \varphi, t)$ is the water displacement and f is the Coriolis parameter. The total grid number on globe is 49 263 361 (10 801×4561) with the 2 min mesh resolution (ETOPO2) and time step used was 5 s. On the land boundaries the reflected condition is applied.

The modeling of the tsunami sources of the volcanic eruption is extremely difficult task and three hypotheses: caldera collapse, submarine explosion and pyrolastic flow are actively considered for the Krakatau event (Francis, 1985). Recently Nomanbhoy and Satake (1995) concluded that the submarine explosion model as the source of the largest tsunami is favored. The global behavior of the tsunami waves during the 1883 Krakatau event should be determined by the

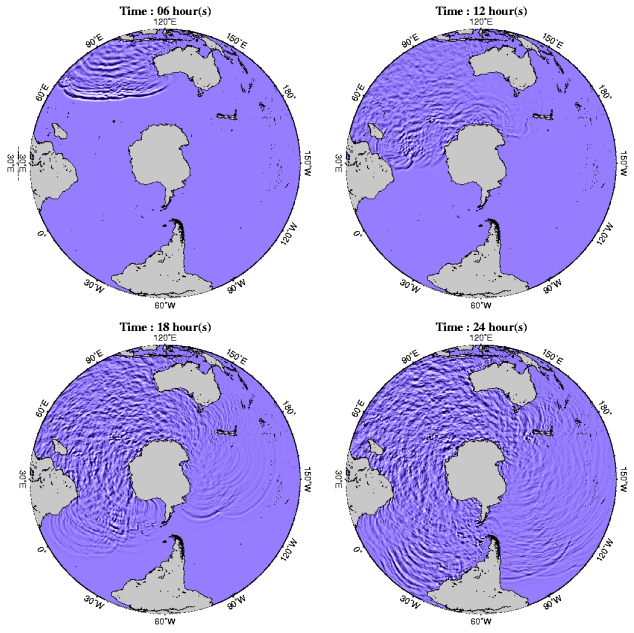

Fig. 8. Snapshots of tsunami propagation with interval of 6 h.

integral characteristics (period, amplitude) on the waves going out the Sunda Strait only, not by the details of tsunami generation. In such cases the conception of the equivalent source can be used, when the real process of the tsunami generating is parametrized by the initial displacement and zero flow distribution. Then the hydrodynamic equations are solved as the Cauchy problem. Such model has been already used for the Krakatau tsunami by Nakamura (1984), and his source is a square of about 44×44 km^2 (four grid points) and depression 0.1 m (in fact, his numerical computation shows that initial disturbance should be characterized by 700 m to explain the observed data in the Sunda Strait). According to Bryant (2001) during the third explosion Krakatau collapsed in on itself, forming a caldera about 270 m deep and with a volume of 11.5 km^3. In our computations, the equivalent source has dimensions 7.2×7.2 km^2 (nine grid points) with the center having coordinates: 6°10′ S and 105°10′ E (depth is of about 400 m), and the initial depression of the shape form is 222 m. Such conditions provide the observed volume 11.5 km^3, but not observed diameter in 6 km; this is related with mesh resolution of the numerical scheme. In fact, the detailed features of the equivalent source should not be very important for tsunami simulation on long distances.

Snapshots of the tsunami propagation are presented in Fig. 8 with the time interval 6 h. These computations are used to determine the characteristics of the wave field on globe. The characteristics of the relative energetic waves (with the crest amplitude more 0.1 m) are given in Table 2. First of all, the results of the calculations of the travel time for the leading wave obtained by the ray tracing method and the hydrodynamic modeling should be compared. Figure 9 shows a quite good agreement between two methods for the first wave arriving. As it is expected, the hydrodynamic modeling should

Table 2. Computed travel time and the maximum crest amplitude

	Arriving Time of Leading Wave, h	Arriving Time of Maximal Wave, h	Maximal crest amplitude, m
Geraldton, Australia	4.3	7.5	1.00
Cossack, Australia	4.6	7.2	1.10
Perth, Australia	4.9	24.0	0.83
Batticaloa, Sri Lanka	5.0	14.6	0.47
Port Blair, Andaman Isl.	5.2	15.1	0.44
Colombo, Sri Lanka	5.3	38.0	0.47
Banjermasin, Kalimantan, Indonesia	6.6	11.1	0.62
Rodriguez lsl., Mauritius	6.8	7.0	0.16
Mauritius lsl.	7.6	7.8	0.77
Bombay, India	9.3	37.2	0.52
Sydney, Australia	11.1	34.8	0.16
Ho Chi Min. Vietnam	11.9	32.2	0.17
Port Elizabeth, South Africa	12.5	13.2	1.19
Auckland, New Zealand	13.3	33.0	0.19
Aden, Yemen	13.6	27.8	0.42
Cape Town, South Africa	13.7	16.9	0.66
Wellington, New Zealand	14.1	34.0	0.19
South Georgia lsl.	17.3	31.7	0.22
Luanda, Angola	18.7	32.0	0.19
Stanley, Falkland Isl.	20.1	33.2	0.16
Lagos, Nigeria	20.3	36.3	0.15
Montevideo, Uruguay	21.2	33.6	0.38
Rio de Janeiro, Brazil	22.0	23.1	0.18
Dakar, Senegal	23.2	31.4	0.13
Belem, Brazil	25.4	36.9	0.14
Halifax, Canada	29.7	36.5	0.13
St. Johns, Canada	29.8	32.9	0.11
New York, USA	30.6	35.8	0.22
Jacksonville, Florida, USA	31.0	35.4	0.11

give largest values for travel time than the ray method for "dark" zones, where waves propagate as the edge waves. For instance, the tsunami traveled to Bombay for 11 h according to the observations; meanwhile the ray method estimated the travel time as 8.6 h. The hydrodynamic modeling gives 9.3 h, close to the observed value. Another example is the tsunami propagation along the Australian coast; the travel time is increased in the hydrodynamic model on 1 h comparing with predictions of the ray theory (but it is not enough for explain the observed travel time).

According to calculations, the first wave is not maximal wave, which arrived significantly later (expect a few of coastal locations: Mauritius and Rodriguez Islands, Port Elizabeth). In some locations, the maximal wave arrives a day later, confirming that the seiche oscillations induced by tsunami may continue 1–2 days. Applied numerical model does not include the bottom friction and wave breaking on the beach (the reflected boundary condition is used for all coastal lines) and this can influence on wave dynamics increasing wave amplitudes for large times as well as the total duration of the tide-gauge record. This important problem of appropriate "land" boundary conditions is not quite well investigated.

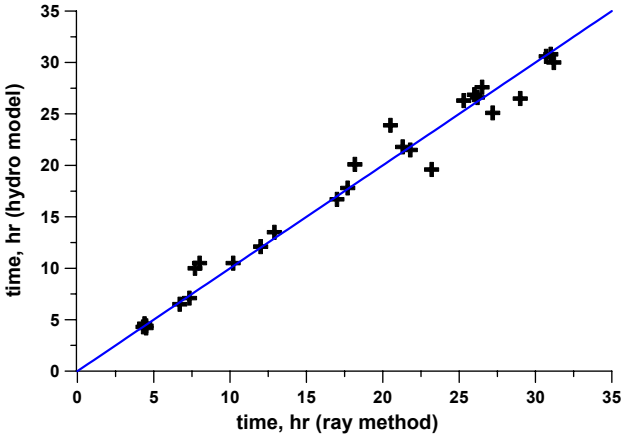

Fig. 9. The comparison of the travel time of the first wave computed by two methods: ray tracing and direct simulation.

Computed wave amplitudes exceed 0.1 m in many locations of the World Ocean, not only in the Indian Ocean

Table 3. Computed and observed tsunami wave amplitudes

	Observed wave amplitude, m	Calculated crest amplitude, m
Cossack, Australia	1.5	1.1
Port Blair, Andaman Isl.	0.2 (tide-gauge)	0.4
Colombo, Sri Lanka	1 (runup)	0.5
Rodriguez lsl., Mauritius	1.8 (runup)	0.2
Mauritius lsl.	0.9 (runup)	0.8
Bombay, India	0.56 (tide-gauge)	0.5
Port Elizabeth, South Africa	0.7 (tide-gauge)	1.2
Auckland, New Zealand	1.5 (runup)	0.2
Aden, Yemen	0.24 (tide-gauge)	0.4
South Georgia Islands	0.3 (tide-gauge)	0.2

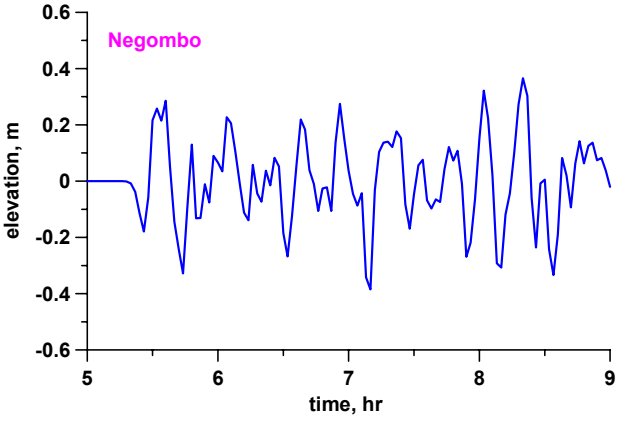

Fig. 10. Computed tide-gauge record for Negombo, Sri Lanka.

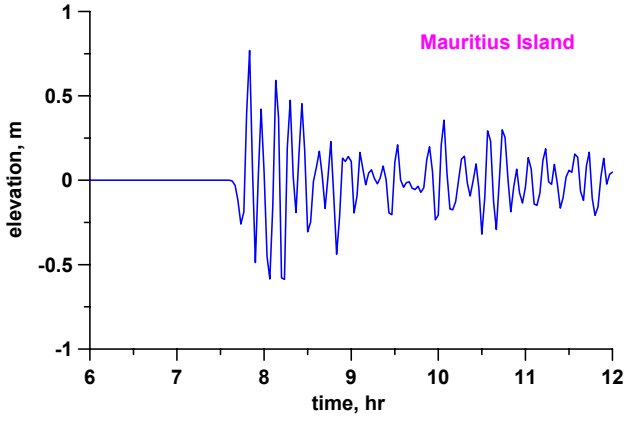

Fig. 11. Computed tide-gauge record for Mauritius Island.

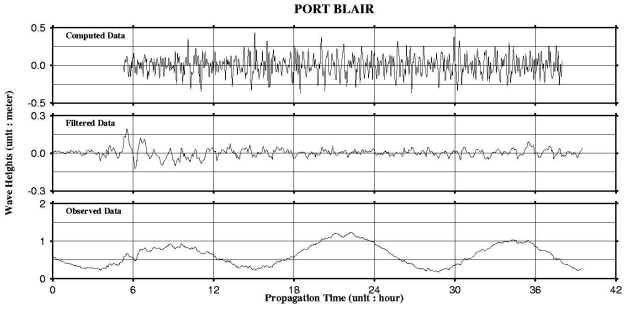

Fig. 12. Comparison of the computed and observed tide-gauge records for Port Blair, Andaman Islands.

(Table 2). For instance, on American Atlantic coast tsunami the amplitudes are 0.1–0.4 m in Canada, USA, Brazil and Uruguay with local highest amplitude 0.38 m in Montevideo. All these locations are in the zone of frontal approaching according to the ray pattern (Fig. 4). Tsunami waves with heights of 0.1–0.2 m are found in calculation for the Atlantic African coast (Senegal, Nigeria and Angola). These locations are in the "dark" zone of the wave rays, and tsunami waves propagate here mainly as the edge waves. It is interesting to mention that the "computed" waves pass through Sunda Strait and have significant amplitudes on the Kalimantan Island (0.62 m). According to the observations tsunami was recorded on many Indonesian Islands in the Java Sea with the height about 0.5–1 m correlated with computed data. The wave reached also Vietnam (0.17 m) but we have no observations for this coast. The rough comparison of the calculated and observed wave amplitudes at several coastal locations is given in Table 3. In average, computed wave amplitudes are in reasonable agreement with observed tide-gauge data, and they are less in several times than the runup heights.

More detail comparison can be done for coastal locations with detail information about tsunami waves: witness reports and tide-gauge records. First of all, the witness reports will be analyzed. According to the observations (Sect. 2), there are about 16 waves during three hours, and the first wave was negative. The computed tide-gauge record for Negombo, Sri Lanka presented in Fig. 10 shows the same features of sea level oscillations during this period. Observed runup height is about 1 m, meanwhile our calculations in the last "sea" point gives 0.4 m only. Such disagreement is typical for comparison of the tide-gauge and runup data. More important is the coinciding of the characteristic wave periods, which is of 10–15 min. The same conclusion can be done for Mauritius Island (Fig. 11), characteristic period is of 15 min. So, the hydrodynamic model explains the observed wave period at different locations in the Indian Ocean.

Simskin and Fiske (1983) have collected tide-gauge records of the Krakatau tsunamis for two locations at the Indian Ocean (Port Blair, India and Port Elizabeth, South Africa), two locations at the Atlantic Ocean (Moltke Harbor, South Georgia Islands and Colon, Panama) and three locations at the Pacific Ocean (Honolulu, San Francisco and Kodial, USA). The quality of these reproduced "paper" records is not quite good to digitize and to analyze. Nevertheless, all these records were digitized and the tide component (calculated by smoothing of real record) was eliminated for comparison with the computed time series. Figure 12 shows re-

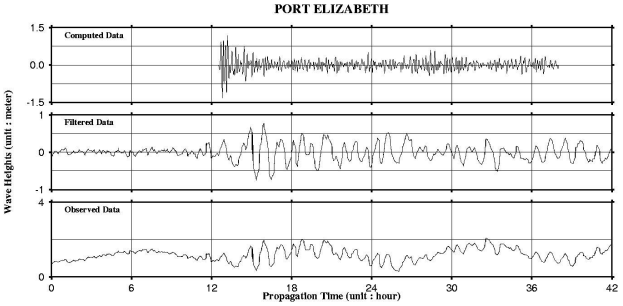

Fig. 13. Comparison of the computed and observed tide-gauge records for Port Elizabeth, South Africa.

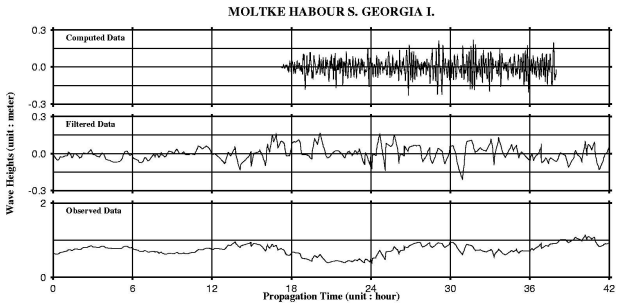

Fig. 14. Comparison of the computed and observed tide-gauge records for Port Moltke, South Georgia Islands.

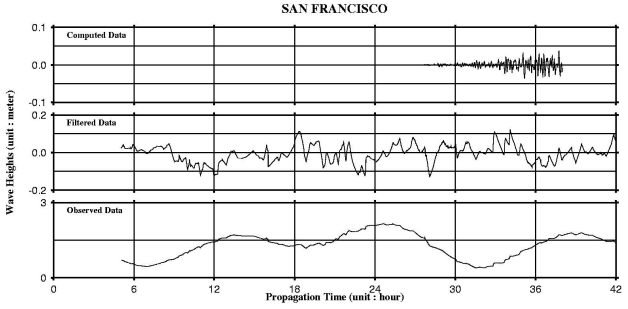

Fig. 15. Comparison of the computed and observed tide-gauge records for San Francisco, USA.

sults of comparison for Port Bair, Andaman Islands. The character of the first (leading) wave in observation and computing is the same (form, arriving time and crest amplitude), but totally the curves are different. First of all, observed tide-gauge record has the characteristic period of 1 h, meanwhile the computed wave record is about 15 min. The large difference in the computed and observed periods needs to be explained. According to the calculations by Nomanbhoy and Satake (1995), the characteristics period of the first two tsunami waves near the Krakatau Island, in the Sunda Strait is about 1 h (but the wave form is far from simplest sine), and, therefore, this low-frequency spectral component should be in the tsunami spectrum on any distance from the source, including the Port Blair. The computed tide-gauge record has the wide spectrum, and this low-frequency component is weak. The characteristic period (15,min) obtained in computing corresponds to the witness reports in all areas of the Indian Ocean, and, therefore, this high-frequency spectral component is also a part of the real spectrum of tsunami. Perhaps, the tide-gauge station eliminates the high-frequency components due to its frequency characteristics. The same difference can be pointed out for Port Elizabeth, South Africa (Fig. 13). The high-frequency computed record has the intense leading group and relative weak seiche oscillations, whereas the observed record contains large low-frequency oscillations during one day. The comparison of the time series with different spectra is impossible. We suggest investigating the influence of frequency filtration (depending from its transfer function) on the waveform for some model and real situations in future.

Comparison of the computed and observed tide-gauge records for Port Moltke, South Georgia Islands Additional problem to compare the computed time series and observed tide-gauge records for the coastal locations in the Atlantic and Pacific Oceans is related with large difference between travel times, see Fig. 14 (Port Moltke, South Georgia Islands) and Fig. 15 (San Francisco). Tsunami waves approached to most of coastal locations significantly early than it is predicted by the hydrodynamic theory (except Le Havre, France, where the comparison is quite well). Almost 50 years ago, based on rough estimates of the travel time, Ewing and Press (1955) suggested that observed sea level disturbances at the coastal locations on American coast are induced by the air-pressure waves generated at the Krakatau eruption in the atmosphere. Our calculations in the framework of the hydrodynamic theory with more accurate bathymetry for all locations mentioned by Ewin and Press (1955) do not rebut their point of view.

5 Discussion and conclusions

The numerical simulation of the tsunami propagated from the Krakatau Island has been done with very high accurate bathymetry from the 2 min ETOPO2 dataset in the framework of the ray tracing method and the direct hydrodynamic theory based on shallow-water equations. Both models demonstrate that tsunami wave penetrate in the Atlantic and Pacific Oceans from the Indian Ocean, and the results of calculations of the travel time within both theories are in good agreement between them. The observed travel times for coastal locations in the Indian Ocean are explained by the computing very well. The observed travel times for other areas of the World Ocean are in contradiction with the theoretical predictions, except Le Havre, France (about 18,000 km from Krakatau). Observed sea level disturbances in New Zealand occurred significantly later (one day) than predicted. Because the water level oscillations observed at this time also in the Lake Taupo (center of the North Island) closed from the sea, our calculations confirm the previous conclusion by Bryant (2001) than these disturbances

were not induced by the Krakatau eruption. Sea level disturbances on the American coast (Honolulu, San Francisco, Kodiak, Colon, Port Moltke), opposite, observed early than it is predicted and, therefore, cannot be induced by the tsunami waves approaching from the Krakatau. The physical mechanism of their appearance is perhaps the "air" mechanism discussed by Ewing and Press (1955), Press and Harkrider (1966) and Garret (1976). Sea level disturbances according to this hypothesis were transferred to the water from the barometric perturbations in the atmosphere. It is based on the almost the same time of wave arriving on barometers and tide-gauges on the American coast. The resonance mechanisms of the tsunami waves by the moving atmospheric disturbances like cyclones are very popular to explain so called meteo tsunamis (Murty, 1977; Pelinovsky, 1996). Very intense acoustic-gravity waves generated by the Krakatau volcanic eruption may have the phase speed comparable with the water wave speed due to the stratification of the earth atmosphere and as a result, there is a coupling between two wave systems. On the shoreline and continental slope the large transformation between waves is possible providing the local disturbances of sea level on tide-gauge stations.

According to the calculations, the tsunami waves are significant in the Indian Ocean having amplitudes exceeded 1 m on the northwestern coast of Australia and southeastern coast of Africa. According to the observations (Sect. 2) the large tsunami waves were observed on all coasts of Indian Ocean: Australia, India, Sri Lanka, Mauritius, and South Africa. Computing explains the ytavel time, observed group character of tsunami waves, and visible wave period (15 min) by witnesses, but not observed tide-gauge (see below). Computed tsunami wave amplitudes in the Java Sea reached 70 cm correlating with observed data in 0.5–1 m.

In the Atlantic Ocean, the computed wave amplitudes exceed 10 cm in South America (South Georgia Islands, Uruguay, Brazil), USA coast (Florida, New York), Canada (Halifax), and African coast (Angola, Nigeria and Senegal). Unfortunately, there is no data of tsunami observation on the eastern coast of USA, Canada and Africa. For South America, there is only one tide-gauge record is available (Port Moltke, Fig. 14), and it shows that tsunami appears early on several hours then predicted. Perhaps, the first sea-level disturbances at Port Moltke were induced by air-pressure waves as it was suggested by Ewing and Press (1955), but the following sea level oscillations were related with approaching of tsunami waves; observed and computed wave amplitudes are in good agreement. For the Caribbean Islands and the English Channel, where some unusual sea level disturbances were observed, computations give weak amplitude waves, less 10 cm.

In the Pacific Ocean, except New Zealand, the computed tsunami waves are too small to compare with observed sea level disturbances in USA and arrived significantly later than observed. As we mentioned, our calculations do not rebut the hypothesis by Ewing and Press (1955) of another origin of observed sea level disturbances. For New Zealand locations computed tsunami amplitude is about 20 cm, but these waves should arrive significantly early than observed sea level disturbances. Our calculations confirm the opinion by Bryant (2001) that tsunami in New Zealand has another origin.

The last conclusion concerns the characteristic periods of the tsunami waves. In computing, the visible period is about 15 min, and this coincides with observations made by witnesses. The observed tide-gauge records have the dominant period of 1 h. The real frequency characteristics of the tide-gauge stations are unknown that to apply any filter procedure to cut parasitic frequencies. We suggest performing special experiments with filtration of tsunami waves in future.

Finally, we may say that the hydrodynamic model explains reasonably the tsunami waves from the Krakatau eruption in the Indian Ocean. Tsunami waves according to calculations may have amplitudes more 10 cm in the Atlantic Ocean, but unfortunately there is no data of tsunami observation in selected locations. Computed tsunami waves are too weak in the Pacific Ocean, except New Zealand, that to induce visible sea level disturbances.

Acknowledgements. This work was supported by the Korean Science and Engineering Foundation (KOSEF) through the Korean Earthquake Engineering Research Center (KEERC) at Seoul National University. Particular support to EP was obtained through RFBR grant 02-05-65107 and EGIBE Program. Thanks are also due to F. Imamura, Tohoku University and K. Satake for providing us with hydrodynamic and ray tracing codes respectively, and Ch. N. Go providing the unpublished manuscript by Soloviev and Go.

References

Bryant, T.: Tsunamis, Cambridge University Press. 2001.

Choi, B. H., Kim, Y. K., and Kim, K. W.: Visualization of a tsunami due to 1883 Krakatau eruption, Proceedings of Korean Computer Graphics Society, 22–26, 1997.

Ewing, M. and Press, F.: Tide-gauge disturbances from the Great Eruption of Krakatoa, Transactions of the AGU, 36, 53–60, 1995.

Francis, P. W.: The origin of the 1883 Krakatau tsunamis, J. Volcanol. Geotherm. Res., 25, 349–369, 1985.

Garret, C. J. R.: A theory of the Krakatoa tide-gauge disturbances, Tellus, 22, 43–52, 1976.

Kawamata, S.; Imamura, F., and Shuto, N.: Numerical simulation of the 1883 Krakatau tsunami, Proceedings of 20th IAHR, Tokyo, Japan, 1992.

Lander, J. F. and Lockridge, P. A.: United States Tsunamis, 1690–1988, National Geophysical Data Center, Boulder, 1989.

Lander, J. F., Whiteside, L. S., and Lockridge, P. A.: A brief history of tsunamis in the Caribbean Sea, Science of Tsunami Hazards, 20, 57–94, 2002.

Murty, T.: Seismic Sea Waves – Tsunamis, Bull. of Dep. Fisheries, Canada, 1977.

Nakamura, S.: A numerical tracking of the 1883 Krakatau tsunami, Science of Tsunami Hazards, 2, 41–54, 1984.

Nomanbhoy, N. and Satake, K.: Generation mechanism of tsunamis from the 1883 Krakatau eruption, Geophys. Res. Letters, 22, 509–512, 1995.

Pelinovsky, E.: Hydrodynamics of Tsunami Waves, Applied Physics Institute Press, Nizhny Novgorod, 1996.

Press , F. and Harkrider, D.: Air-Sea Waves from the Explosion of Kralatoa, Science, 154, 1325–1327, 1966.

Satake, K.: Effects of Bathymetry on Tsunami Propagation: Application of Ray Tracing to Tsunamis, PAGEOPH, 126, 27–36, 1988.

Simskin, T. and Fiske, R. S.: Krakatau 1883 – the volcanic eruption and its effects, Smithsonian Institution Press, Washington, D. C., 1983.

Smith, W. H. F. and Sandwell, D. T.: Global Sea Floor Topography from satellite altimetry and Ship depth soundings, Science,, 277, 5334, 1997.

Sobel, P. A. and von Seggern, D. H.: Application of surface-wave ray tracing, Bull. of Seism. Soc. Am., 68, 1359–1380, 1978.

Soloviev, S. L. and Go, Ch. N.: Catalog of tsunamis in western coast of the Pacific Ocean, Moscow: Nauka, 1974.

USSR Navy: Pacific Ocean (Series of the Atlases of the Oceans), Moscow, 1974.

Yokoyama, I.: A geophysical interpretation of the 1883 Krakatau eruption, J. Volcanology and Geothermal Research, 9, 359–378, 1981.